6-15-2009

A Hybrid Biofuel Cell Based on Electrooxidation of Glucose Using Ultra-Small Silicon Nanoparticles

Yongki Choi
City University of New York

Gang Wang
Cleveland State University

Munir H. Nayfeh
University of Illinois at Urbana-Champaign, m-nayfeh@uiuc.edu

Siu-Tung Yau
Cleveland State University, s.yau@csuohio.edu

Publisher's Statement

NOTICE: this is the author's version of a work that was accepted for publication in Biosensors & Bioelectronics. Changes resulting from the publishing process, such as peer review, editing, corrections, structural formatting, and other quality control mechanisms may not be reflected in this document. Changes may have been made to this work since it was submitted for publication. A definitive version was subsequently published in Biosensors & Bioelectronics, 24, 10, (06-15-2009); 10.1016/j.bios.2009.03.032

Original Citation

Choi, Y., Wang, G., Nayfeh, M. H., , & Yau, S. (2009). A hybrid biofuel cell based on electrooxidation of glucose using ultra-small silicon nanoparticles. Biosensors and Bioelectronics, 24(10), 3103-3107. doi:10.1016/j.bios.2009.03.032

Repository Citation

A hybrid biofuel cell based on electrooxidation of glucose using ultra-small silicon nanoparticles

Yongki Choi[a,b], Gang Wang[a], Munir H. Nayfeh[c,*], Siu-Tung Yau[a,**]

[a] Department of Electrical and Computer Engineering, Cleveland State University, 2121 Euclid Ave., Cleveland, OH 44115, USA
[b] Department of Physics, Graduate Center of City University of New York, New York, NY 10016-4309, USA
[c] Department of Physics, University of Illinois at Urbana-Champaign, Urbana, IL 61801, USA

1. Introduction

Enzymatic biofuel cells convert chemical energy stored in organic fuels directly to electrical energy using enzymes as catalysts for both the anode and the cathode reactions. Because of enzymes' specificities for their substrates, the fuel and the oxidant can be contained in a single compartment without using a membrane to separate them as is the case with the conventional fuel cell (Katz et al., 2003). This feature, which allows device miniaturization, makes the single-compartment biofuel cell outplay the conventional fuel cell in the area of implantable power source for biomedical applications (CalabreseBarton et al., 2004; Heller, 2004). It is envisaged that, using physiologically ambient glucose as fuel, the biofuel cell can be used as power supply for biosensors (CalabreseBarton et al., 2004; Heller, 2004), cardiac pacemakers (Holmes, 2003), prosthetic applications such as artificial hearing (Rauschecker and Shannon, 2002) or vision (Maynard, 2001), or the process of functional electrical stimulation (Bhadra et al., 2001; Craelius, 2002). A typical power level of ~1 μW is required for the operation of the cardiac pacemaker (Linden and Reddy, 2002). However, two critical issues exist in the present development of biofuel cells, namely, output power density and cell stability (CalabreseBarton et al., 2004). For implantable uses, the output of biofuel cells should be stable under long-term, *in vivo* conditions. The short lifetime of present prototype biofuel cells is due to the instability of enzymes (Pizzariello et al., 2002; Takeuchi and Amao, 2004).

Katz et al. (1999) have demonstrated a single-compartment glucose fuel cell. The anode consisted of reconstituted glucose oxidase (GOx), which catalyzed the oxidation of glucose. The cathode consisted of cytochrome oxidase (COx) coupled to cytochrome *c* for the reduction of O_2. Operating the cell in an air-saturated solution containing 1 mM glucose at pH 7 and at 25 °C produced 4 μW. Heller and co-workers have developed a miniature single-compartment biofuel cell (Chen et al., 2001). A GOx-immobilized carbon fiber anode catalyzed the oxidation of glucose and a laccase-immobilized carbon fiber cathode reduced O_2. Both electrodes were covered with a redox hydrogels as electron transfer mediators. The cell was operated in a pH 5 citrate buffer, which contained 15 mM glucose and was saturated with air. The cell produced peak power densities of 64 and 137 μW/cm^2 at 23 and 37 °C, respectively. The output current decreased by 25% over 3 days.

Because of their inherent instability, enzymes become unstable under the non-native conditions of the fuel cell environment, making long-term applications unattainable (CalabreseBarton et al., 2004). In a recent study, we have demonstrated that ultra-small silicon nanoparticles behave as an electrocatalyst for the oxidation of glucose (Choi et al., 2008; Wang et al., 2006). The particles, compared to the enzyme GOx, showed fast substrate conversion kinetic characteristics and particle-immobilized electrodes exhibited stable long-term current output. In this article, we first present an

electrochemical characterization of the oxidation of glucose catalyzed by the silicon particle. The characterization shows that the onset of the oxidation occurs at −0.4 V vs. Ag/AgCl (−0.62 V vs. RHE) at neutral pH. The oxidation appears to be a first order reaction which involves the transfer of 1 electron. To demonstrate the potential of the particle in implantable power, we have used it as the anode catalyst to construct a prototype single-compartment hybrid biofuel cell, which operated on glucose and hydrogen peroxide (H_2O_2). A peak power density of 1.4 $\mu W/cm^2$ was obtained with the enzyme horseradish peroxidase (HRP) used as the cathode catalyst. The power density was optimized to 3.7 $\mu W/cm^2$ when HRP was replaced by microperoxidase-11 (MP-11). The long-term stability of the cell was characterized by monitoring the cell voltage for 5 days. A comparison between the hybrid cell and a biofuel cell shows that the hybrid cell provides a much better performance in terms of output power density and stability presumably due to fast kinetics and the robustness of the silicon particle.

2. Materials and methods

The silicon nanoparticles were made by electrochemical etching of a (1 0 0)-oriented p-type (1–10 Ω cm) silicon wafer in hydrofluoric acid and hydrogen peroxide. The silicon wafer anode, placed at a certain distance from a platinum cathode, was anodized with a constant current (150 mA) while being vertically immersed in the etchant at a reduced speed of ~1 mm per hour. The anodized wafer was then transferred to an ultrasound bath containing either water or an organic solvent such as benzene, isopropyl alcohol or tetrahydrofuran (THF) for a brief treatment, which resulted in crumbling of particles from the wafer into the solvent to form a colloid suspension (Belomoin et al., 2000). This etching technique can be used to prepare 1-nanometer particles (Si1) and 2.8-nanometer particles (Si2.8), depending on etching conditions. Monte Carlo simulation of the Si1 particle suggests a filled fullerene structure of $Si_{29}H_{24}$, in which a central core silicon atom and four other silicon atoms are arranged in a tetrahedral coordination and the 24 remaining silicon atoms undergo a H-terminated bulk-like (2 × 1) reconstruction of dimer pairs on (0 0 1) facets (6 reconstructed surface dimers) (Rao et al., 2004). The particles exhibit interesting optical properties such as luminescence in the visible part of the spectrum (Belomoin et al., 2000), second harmonic generation (Nayfeh et al., 2000) and laser oscillation (Nayfeh et al., 2002). Under UV excitation, the Si1 particle generates blue spontaneous emission with a measured band-gap of 3 eV and the Si2.8 particle generates red emission with a 2 eV band-gap (Rao et al., 2004). Figure S1A (see Supplementary materials) shows the spontaneous emission of the two kinds of silicon particles. Figures S1B and S1C (see Supplementary materials) are the electron micrographs of the particles.

The particle used in this work was benzene-based Si1 (molecular weight = 838.8) colloid with a concentration of 10 μM. Glucose (β-D(+)glucose, G5250, Sigma), microperoxidase-11 (M6756, Sigma), horseradish peroxidase (P8375, Sigma), and GOx (G6125, Sigma) were used as received. Other chemicals used in this work were of analytical grade. Deionized water (ρ = 18.2 MΩ cm, Direct Q3, Millipore) was used to prepare solutions. Phosphate buffer solution (PBS, 100 mM) was prepared for general use. Heavily doped (ρ < 0.005 Ω cm) n-type silicon wafers (Virginia Semiconductor, USA) and highly oriented pyrolytic graphite (HOPG, SPI, USA) were used to support the silicon particles and enzymes as electrodes.

Si1 particles were immobilized on silicon and HOPG. The silicon wafer with its surface containing the native oxide was cleaned with ethanol, isopropanol, and deionized water. A 0.1 ml drop of the Si1 colloid was spread on the wafer surface, and the sample was incubated in a container under moisture for 10 h and then rinsed with deionized water. The surface of the particle-immobilized wafer was covered with a mask to form the Si1–Si electrode with a working area of about 1 mm × 1 mm. The particle-immobilized HOPG (Si1-HOPG) electrode was prepared by depositing the particle on the basal plane of HOPG followed by incubation. The Si1-HOPG electrode had a surface area of 2 mm × 5 mm. The enzymes (HRP, MP-11, and GOx) were immobilized on the edge plane of HOPG (epHOPG). HOPG sheets (2 mm × 5 mm) were polished to expose the edge plane (Strauss et al., 2004). Enzyme solutions were made by dissolving 1 mg of the respective enzyme in 1 ml of 20 mM PBS at pH 7.0. A 0.1 ml drop of the enzyme solution was deposited on the epHOPG, which was then incubated at room temperature for 4 h. The electrode was then rinsed with deionized water. Previously, it has been demonstrated that enzymes are able to retain their bioactivities when immobilized on the epHOPG electrodes (Armstrong et al., 1989; Strauss et al., 2004; Wang and Yau, 2006).

Electrochemical measurements were performed with a 1-ml conventional three-electrode cell, controlled by a potentiostat (CH Instrument 660C, Austin, USA). A Si1–Si, HRP-epHOPG or MP-11-epHOPG electrode was used as the working electrode. A commercial Ag/AgCl (3 M KCl) electrode was used as the reference electrode, and a platinum wire was used as the counter electrode. Cyclic voltammetry was performed at a potential scan rate of 20 mV/s in solutions prepared with a PBS at pH 7. The PBS was deaerated by purging with pure nitrogen gas. Tafel measurements were performed at 1 mV/s. The Tafel plot is used to determine kinetic parameters of an electrochemical reaction. In our work, we use it to estimate the number of electron transferred in the oxidation of glucose. A Tafel plot is obtained by measuring the logarithm of the current or current density of a working electrode while varying the overpotential. In a typical Tafel plot generated using a commercial potentiostat, the vertical axis represents the total potential E applied to the working electrode and the overpotential is the difference between the equilibrium potential, the potential at which no or very little current flows, and the total applied potential E.

For fuel cell measurements, the Si1-HOPG electrode and the GOx-epHOPG electrode were used as anodes and the HRP-epHOPG and the MP-11-epHOPG electrodes were used as cathodes. A circuit was built to provide different load resistances in the external circuit. The fuel cell working solution was a 20 mM phosphate buffer containing 0.1 M KCl and glucose at different concentrations. The solution was not deaerated. The cell current and the cell voltage between the electrodes were measured with a multimeter (K2000, Keithley Instruments, Cleveland, USA). All electrochemical experiments were carried out at 20 ± 0.5 °C.

3. Results and discussion

3.1. Particle-catalyzed electrooxidation of glucose

We have performed cyclic voltammetry of the Si1–Si electrode to study the catalytic properties of Si1 for glucose oxidation. The cyclic voltammograms (CV) that indicate the particle-catalyzed electrooxidation of glucose at pH 7 are shown in Fig. 1A. The CV (black dashed) obtained with a bare silicon electrode in PBS without glucose coincides with that (blue dash-dotted) obtained with the same electrode in the presence of glucose. The green dotted CV is the background signal of the Si1–Si electrode obtained in PBS. When glucose was added to the PBS resulting in a 2 mM solution, the response of the electrode is indicated by the red solid CV, which shows an increase in the anodic current above the background. This increase indicates the direct oxidation of glucose by the electrode. Note that the bare silicon wafer shows no response to glucose within the range of potential used in the experiment. Thus, the solid CV indicates the electrooxidation of glucose catalyzed by Si1. Shown in the inset of Fig. 1A is the glucose calibration curve of the electrode obtained at pH 7.

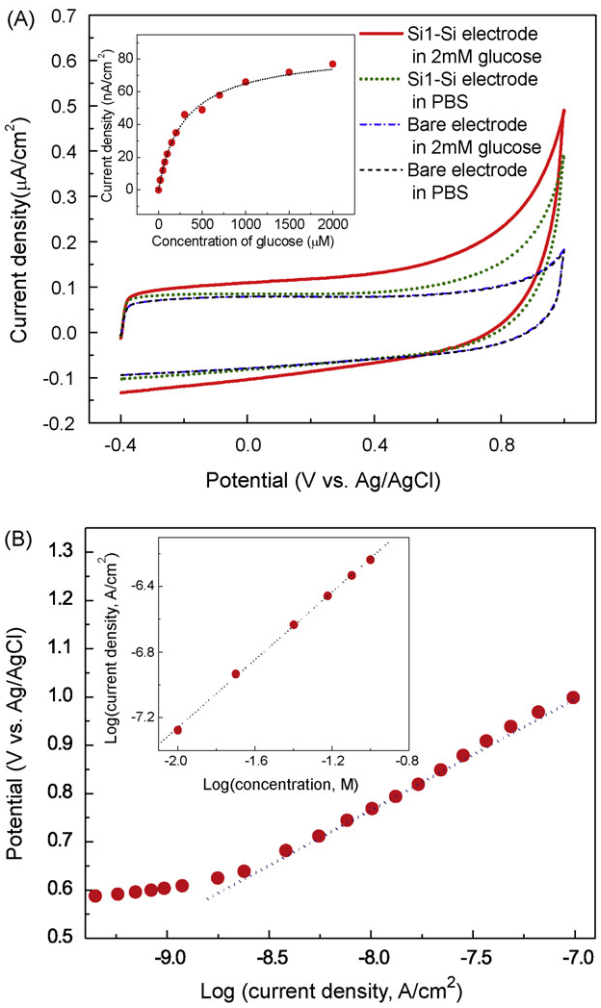

Fig. 1. Electrooxidation of glucose using the Si1–Si electrode. (A) The dashed CV was obtained with a bare silicon electrode in PBS without glucose while the dash-dotted CV was obtained with the same electrode in the presence of 2 mM glucose. The dotted CV, the background signal, was obtained with the electrode in a 50 mM PBS at pH 7. The solid CV is the electrode's response to adding 2 mM glucose to the PBS. The inset shows the electrode's glucose calibration curve obtained at 0.8 V at pH 7. Each data point shows the oxidation current obtained by subtracting the background current from the total anodic current. (B) The Tafel plot of the Si1–Si electrode in 20 mM of glucose. The plot was obtained at 1 mV/s. The dotted straight line is used to determine the Tafel slope, which is equal to 181 mV/decade. The inset is a semi-log plot of the electrode's oxidation current density vs. glucose concentration obtained at 0.8 V of the Tafel plot. The semi-log plot is used to determine the reaction order.

Several characteristics of the catalytic process should be noted. The oxidation, as shown by the solid CV of Fig. 1A, occurs at potentials as low as −0.40 V vs. Ag/AgCl (−0.62 V vs. RHE). The glucose calibration curve of the electrode is linear in the low concentration range, followed by a saturation region for higher glucose concentrations. This shape resembles those of enzymes and is indicative of the Michaelis–Menten kinetics. To characterize the kinetic properties of the oxidation, we have obtained Tafel plots of the particle-immobilized electrode. Fig. 1B shows the Tafel plot of a Si1–Si electrode obtained in 20 mM glucose solution at pH 7. The Tafel slope yields the value of the product, αn, where α is the electron transfer coefficient and n is the number of electrons transferred per molecule (Bard and Faulkner, 2001). Fig. 1B shows that, with the slope being 181 mV/decade, the value of αn is 0.33, suggesting a most probable value of $n = 1$ for the catalysis. The inset shows the logarithmic plot of oxidation current density as a function of glucose concentration at a constant electrode potential. The slope

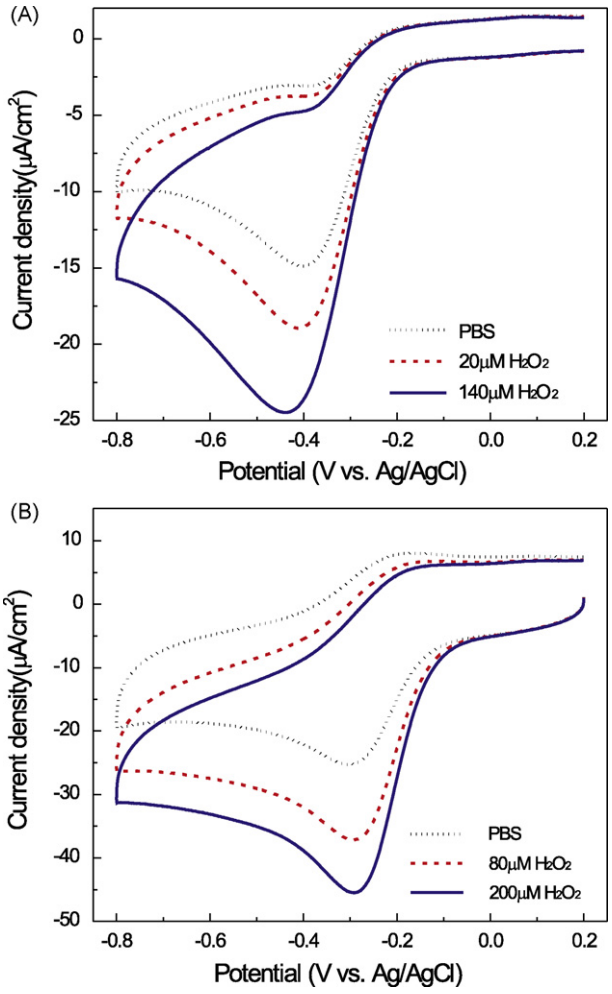

Fig. 2. Electro-reduction of H_2O_2 catalyzed by HRP and MP-11. (A) The CVs were obtained with a HRP-immobilized epHOPG electrode in PBS and in two different H_2O_2 concentrations. (B) The CVs were obtained with a MP-11-immobilized epHOPG electrode in PBS and in two different H_2O_2 concentrations. MP-11 produced more reduction current and a more positive reduction onset potential.

of the plot yields the order of the catalytic reaction, which is 1.07. Thus, the electrooxidation of glucose as catalyzed by Si1 is a first order reaction which involves the transfer of 1 electron. Possible products of the oxidation of glucose observed here include different kinds of carboxylic acids as previously observed on platinum electrodes (Kokoh et al., 1992). Future work includes identifying the products.

3.2. The hybrid fuel cell

To demonstrate the potential of the silicon nanoparticle, we have constructed a hybrid biofuel cell using the nanoparticle as the anode catalyst. Figure S2 (see Supplementary materials) is a schematic description of the fuel cell. The anode was an epHOPG immobilized with Si1 and the cathode was an epHOPG immobilized with HRP. The anode and cathode were immersed in a PBS contained in a beaker and electrically connected through a load resistance R_L. This prototype single-compartment fuel cell operated on glucose and H_2O_2, which were dissolved in the PBS. Glucose was oxidized by Si1 and H_2O_2 was reduced by HRP. It is known that HRP in the presence of an electron donor catalyzes the reduction of H_2O_2 to water (Mathews et al., 2000). The CVs in Fig. 2A show the bio-electroreduction of H_2O_2 brought about using a HRP-immobilized epHOPG electrode. The CVs indicate that the onset of the reduction

occurs at −0.15 V vs. Ag/AgCl. Note that the particle-catalyzed oxidation of glucose occurs at or below −0.4 V vs. Ag/AgCl as shown in Fig. 1. Thus, the reduction reaction occurs at a higher potential than the oxidation reaction and the electrode potentials satisfy the requirement for the operating condition of fuel cells.

The hybrid fuel cell was tested with a PBS containing 2 mM glucose and 2 mM H_2O_2 at pH 7 and 20 °C. Fig. 3A shows the cell voltage vs. cell current (*V–I*) and the power density vs. cell current (*P–I*) characteristics of the cell. The open-circuit voltage (V_{oc}) is 0.16 V. The peak power density is 1.3 μW/cm^2. Fig. 3A indicate that the *V–I* characteristics of the hybrid fuel cell deviate from the ideal rectangular behavior (Bockris and Srinivasan, 1969). The deviation shows the typical three-region characteristics: the activation polarization in the low current region, the Ohmic polarization region and the concentration polarization region in higher current regions (Li, 2006). The deviation reduces cell voltage below its reversible thermodynamic value (Mano et al., 2002).

To improve the output power of the hybrid cell, we replaced HRP by the heme-containing polypeptide microperoxidase-11 (MP-11) to reduce H_2O_2 at the cathode. Compared to HRP, MP-11 has a more compact structure, which allows effective direct electrical communication with electrodes as evidenced by the enhanced reduction current shown in Fig. 2B. The MP-11-catalyzed reduction of H_2O_2 also shows a more positive onset of −0.05 V vs. Ag/AgCl. Figure S3 (see Supplementary materials) shows the electrode potential vs. substrate concentration curves of the hybrid cell. The saturation of the curves at high concentrations indicates the Nernstian behavior. The saturated potential values reflect an open-circuit voltage of 0.33 V. The curves can be used to optimize the cell performance.

Fig. 3B shows the *V–I* characteristics of the fuel cell obtained at 2 mM glucose and several concentrations of H_2O_2 and Fig. 3C shows the corresponding *P–I* characteristics. The characteristics corresponding to the condition of 2 mM glucose and 2 mM H_2O_2 are to be compared to those obtained with HRP as shown in Fig. 3A. Note that the remaining three characteristics in Fig. 4B and C were obtained under the physiological concentrations of glucose and H_2O_2 (Mueller et al., 1997). Fig. 3B and 3C show that the output power increases with increasing concentration of H_2O_2 with a glucose concentration of 2 mM. This behavior qualitatively agrees with the result shown in Figure S3 (see Supplementary materials). Fig. 3B indicates that the region of activation polarization is absent in the *V–I* characteristics. We attribute this absence to the enhanced direct electrical communication at the cathode caused by the use of MP-11. The improvement in cell performance is reflected in V_{oc} of 0.28 V, which is close to the predicted value of 0.33 V (see above), and the peak power density of 3.7 μW/cm^2.

We have also constructed a biofuel cell by replacing the anode of the hybrid fuel cell with a GOx-immobilized epHOPG and using MP-11 as the cathode catalyst. Note that the enzymes are in direct contact to the bare electrode (Wang and Yau, 2006). The *V–I* and *P–I* characteristics of the biofuel cell obtained at 2 mM glucose and 2 mM H_2O_2 are shown in Fig. 3D. The *V–I* characteristics shows the three characteristic regions due to deviation from the Nernstian behavior. The peak power density of the biofuel cell is about 5 times less than that obtained with the hybrid fuel cell. Previously, the kinetic properties of the electrooxidation of glucose catalyzed by the particle-immobilized electrode have been compared those catalyzed by the GOx-immobilized electrode (Wang et al., 2006). It was found that the silicon particle is more efficient than GOx in performing the oxidation of glucose with enhanced kinetic rate constants. We attribute the improved performance of the hybrid fuel cell as compared to that of the biofuel cell observed in this work to the enhanced kinetic properties of the particle-catalyzed glucose oxidation. Note that the current and power levels of the biofuel cell at the physiological concentrations (2 mM glucose and

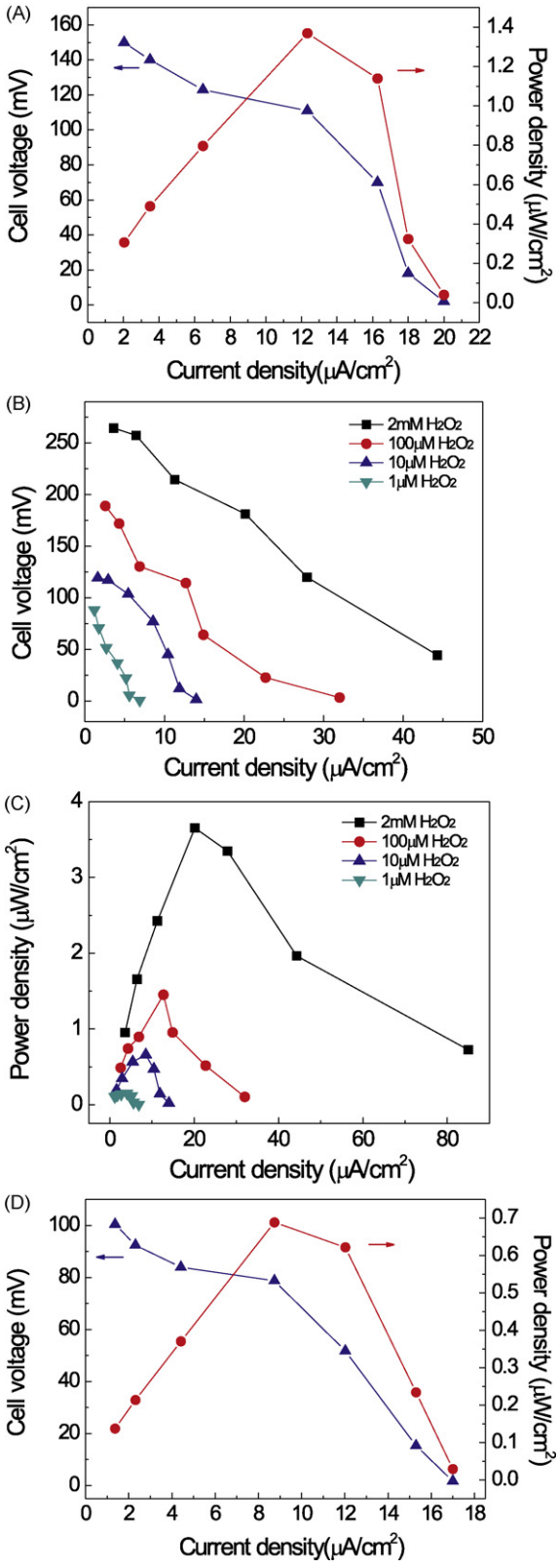

Fig. 3. Characteristics of hybrid biofuel cells and a biofuel cell. (A) The *V–I* and *P–I* characteristics of the hybrid cell with a HRP-epHOPG cathode operating on 2 mM glucose and 2 mM H_2O_2. (B and C) Show the *V–I* and *P–I* characteristics of the hybrid cell with a MP-11-epHOPG cathode operating on 2 mM glucose and different H_2O_2 concentrations. (D) The *V–I* and *P–I* characteristics of a biofuel cell with a GOx-epHOPG anode and a MP-11-epHOPG cathode operating on 2 mM glucose and 2 mM H_2O_2.

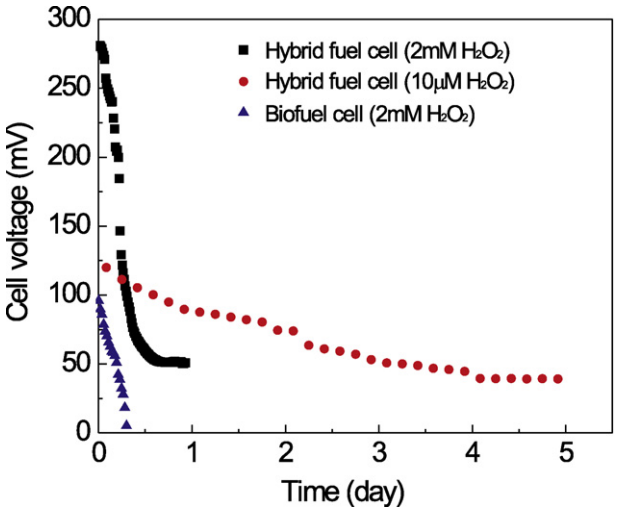

Fig. 4. The stability of the hybrid fuel cell and the biofuel cell as demonstrated by monitoring the cell voltage in time. Both cells contained 2 mM glucose. The hybrid cell contained physiological concentration of H_2O_2 (10 μM).

less than 1 mM H_2O_2) are extremely low compare to those of the hybrid cell as shown in Figs. 3B and 3C.

3.3. *Long-term characterization of the hybrid fuel cell*

The long-term stability of the hybrid fuel cell has been characterized by monitoring the cell voltage for R_L = 1 MΩ. Monitoring the cell voltage using a large load resistance (Ramanavicius et al., 2005) eliminates the effect of the depletion of fuel and oxidizer. Fig. 4 shows the changes in the cell voltage during a period of 5 days at the fuel concentrations giving maximum power (2 mM glucose and 2 mM H_2O_2) and at the physiological concentrations (2 mM glucose and 10 μM H_2O_2). The plot for 2 mM glucose and 2 mM H_2O_2 shows a fast decrease in the cell voltage (82% of the initial value) during the first day. The plot corresponding to the physiological concentrations shows a slow decrease in the cell voltage from its initial value at an average rate of 13% per day. Also shown in Fig. 4 is the time plot of the cell voltage of the biofuel cell operating on 2 mM glucose and 2 mM H_2O_2. The cell voltage dropped to an extremely small value within 8 h. Since the depletion of fuel and oxidizer can be ruled out, the decrease in the cell voltage of the biofuel cell is likely to be caused by the degradation of the enzymes due to the fact that the enzymes are subjected to a non-native environment, i.e. the solution and the electrode. In particular, the presence of H_2O_2 may produce detrimental effects on the enzymes since it is known that H_2O_2 damages cells and tissues. This possibility is supported by the results shown in Fig. 4 that, for the hybrid fuel cell, the voltage in the high H_2O_2 concentration case decrease much faster than in the low H_2O_2 concentration case. This could be due to the detrimental effect of H_2O_2 on MP-11. However, the even faster decrease in the biofuel cell case indicates that H_2O_2 could also make a detrimental effect on GOx, the anode catalyst. Therefore, the improved electrode stability of the hybrid cell compared to biofuel cell could be attributed to the integrity of the silicon particles.

4. Conclusions

An electrochemical study of the electro-oxidation of glucose catalyzed by ultra-small silicon nanoparticles shows that the oxidation is characterized by a onset potential as low as −0.4 V vs. Ag/AgCl (−0.62 V vs. RHE). The oxidation appears to be a first order reaction which involves the transfer of 1 electron. A prototype hybrid biofuel cell that operates on glucose and H_2O_2 has been constructed using the particle as the anode catalyst. It was observed that the hybrid cell's output power can be improved by replacing HRP with MP-11 as the cathode catalyst. A biofuel cell has been constructed and tested. Under identical conditions, the hybrid cell delivers an output power which is more than 5 times larger than that produced by the biofue cell. This observation is most likely to be due to the fast reaction kinetics caused by the silicon particle as previously noticed (Wang et al., 2006). The hybrid cell's long-term stability has been characterized by monitoring the cell voltage for 5 days. Comparing the long-term cell voltage of the hybrid cell to that of the biofuel cell indicates that the hybrid cell has a higher stability. Thus, we conclude that the use of the ultra-small silicon nanoparticle in biofuel cells is a promising approach to address the two critical issues, namely, output power and cell stability, in the present development of biofuel cells.

Acknowledgements

This work was supported by American Diabetes Association (Grant number 7-08-RA-191) and Cleveland State University (Research Challenge Award).

Appendix A. Supplementary data

Supplementary data associated with this article can be found, in the online version, at doi:10.1016/j.bios.2009.03.032.

References

Armstrong, F.A., Bond, A.M., Hill, H.A.O., Psalti, I.S.M., Zoski, C.G., 1989. J. Phys. Chem. 93, 6485–6493.
Bard, A.J., Faulkner, L.R., 2001. Electrochemical Methods, 2nd ed. John Wiley & Sons, Inc., Hoboken, NJ.
Belomoin, G., Therrien, J., Nayfeh, M., 2000. Appl. Phys. Lett. 77, 779–781.
Bhadra, N., Kilgore, K.L., Peckham, P.H., 2001. Med. Eng. Phys. 23, 19–28.
Bockris, J.O.M., Srinivasan, S., 1969. Fuel Cells. McGraw-Hill, New York.
CalabreseBarton, S., Gallaway, J., Atanassov, P., 2004. Chem. Rev. 104 (10), 4867–4886.
Chen, T., Barton, S.C., Binyamin, G., Gao, Z.Q., Zhang, Y.C., Kim, H.H., Heller, A., 2001. J. Am. Chem. Soc. 123 (35), 8630–8631.
Choi, Y., Wang, G., Nayfeh, M.H., Yau, S.-T., 2008. Appl. Phys. Lett. 93, 164103.
Craelius, W., 2002. Science 295, 1018–1021.
Heller, A., 2004. Phys. Chem. Chem. Phys. 6 (2), 209–216.
Holmes, C.F., 2003. Electrochem. Soc. Interface 12, 26–29.
Katz, E., Shipway, A.N., Wilner, I., 2003. In: Vielstich, W., Gasteiger, H.A., Lamm, A. (Eds.), Handbook of Fuel Cells—Fundamentals Technology and Applications. John Wiley & Sons.
Katz, E., Willner, I., Kotlyar, A.B., 1999. J. Electroanal. Chem. 479 (1), 64–68.
Kokoh, K.B., Leger, J.-M., Benden, B., Lamy, C., 1992. Electrochim. Acta 37, 1333–1342.
Li, X., 2006. Principles of Fuel Cells, first ed. Taylor & Francis, New York.
Linden, D., Reddy, T.B., 2002. Handbook of Batteries, third ed. McGraw-Hill, New York.
Mano, N., Mao, F., Heller, A., 2002. J. Am. Chem. Soc. 124 (44), 12962–12963.
Mathews, C.K., Hold, K.E.v., Ahern, K.G., 2000. Biochemistry, third ed. Addison Wesley Longman, Inc., San Francisco.
Maynard, E.M., 2001. Annu. Rev. Biomed. Eng. 3, 145–168.
Mueller, S., Riedel, H.-D., Stremmel, W., 1997. Anal. Biochem. 245, 55–60.
Nayfeh, M.H., Akcakir, O., Belomoin, G., Barry, N., Therrien, J., Gratton, E., 2000. Appl. Phys. Lett. 77, 4086–4088.
Nayfeh, M.H., Rao, S., Barry, N., Therrien, J., Belomoin, G., Smith, A., Chaieb, S., 2002. Appl. Phys. Lett. 80, 121–123.
Pizzariello, A., Stred'ansky, M., Miertus, S., 2002. Bioelectrochemistry 56 (1-2), 99–105.
Ramanavicius, A., Kausaite, A., Ramanaviciene, A., 2005. Biosens. Bioelectron. 20, 1962–1967.
Rao, S., Sutin, J., Clegg, R., Gratton, E., Nayfeh, M.H., Habbal, S., Tsolakidis, A., Martin, R.M., 2004. Phys. Rev. B 69, 205319.
Rauschecker, J.P., Shannon, R.V., 2002. Science 295, 1025–1029.
Strauss, E., Thomas, B., Yau, S.-T., 2004. Langmuir 20, 8768–8772.
Takeuchi, Y., Amao, Y., 2004. J. Jpn. Petrol. Inst. 47 (5), 355–358.
Wang, G., Mantey, K., Nayfeh, M.H., Yau, S.-T., 2006. Appl. Phys. Lett. 89, 243901.
Wang, G., Yau, S.-T., 2006. Electrochem. Commun. 8, 987–992.